

A Complete Sample of Soft X-ray Selected AGN: I. The Data¹

Dirk Grupe^{2,3}

Astronomy Department, Ohio State University, 140 W. 18th Ave., Columbus, OH-43210, U.S.A.
dgrupe@astronomy.ohio-state.edu

Beverley J. Wills⁴

Astronomy Department, University of Texas at Austin, RLM 15.308, Austin, TX 78712, U.S.A.
bev@pan.as.utexas.edu

Karen M. Leighly⁵

Dept. of Physics and Astronomy, University of Oklahoma, 440 W. Brooks St., Norman, OK 73019, U.S.A.
leighly@nhn.ou.edu

Helmut Meusinger⁶

Thüringer Landessternwarte Tautenburg, Sternwarte 5, D-07778 Tautenburg, Germany

ABSTRACT

We present the optical spectra and simple statistical analysis for a complete sample of 110 soft X-ray selected AGN. About half of the sources are Narrow-Line Seyfert 1 galaxies (NLS1s), which have the steepest X-ray spectra, strongest FeII emission and slightly weaker [OIII] λ 5007 emission than broad line Seyfert 1s (BLS1s). Kolmogorov Smirnov tests show that NLS1s and BLS1s have clearly different distributions of the X-ray spectral slope α_X , X-ray short-term variability, and FeII equivalent widths and luminosity and FeII/H β ratios. The differences in the [OIII]/H β and [OIII] equivalent widths are only marginal. We found no significant differences between NLS1s and BLS1s in their rest frame 0.2-2.0 X-ray luminosities, rest frame 5100Å monochromatic luminosities, bolometric luminosities, redshifts, and their H β equivalent widths.

Please note: this is a special version for astro-ph that does not contain the optical and FeII subtracted spectra. The complete paper including the spectra can be retrieved from http://www.astronomy.ohio-state.edu/~dgrupe/research/sample_paper1.html

Subject headings: galaxies: active - quasars:general

¹Based in part on observations at the European Southern Observatory La Silla (Chile) with the 2.2m telescope of the Max-Planck-Society during MPI and ESO time, and the ESO 1.52m telescope during ESO time in September 1995 and September 1999.

²Guest observer, McDonald Observatory, University of Texas at Austin

1. Introduction

With the launch of the X-ray satellite ROSAT (Trümper (1982)) a new chapter in the history of astronomy was written. With the spectral sensitivity of the Position Sensitive Proportional Counter (PSPC, Pfeffermann et al. (1987)) to energies as low as 0.1 keV it was possible for the first time to study the soft X-ray properties of a large number of AGN. In the first half year of its mission

ROSAT performed, for the first time, an all-sky survey (RASS, Voges et al. (1999)) in the 0.1-2.4 keV energy band. This survey led to the discovery of a large number of previously unknown soft X-ray sources (Thomas et al. (1998); Beuermann et al. (1999); Schwobe et al. (2000)), about 1/3 of them AGN. Many AGN show a strong excess in soft X-rays. Most of their bolometric luminosity is emitted in the energy range between the UV and soft X-ray energies. It is commonly believed that this 'Big Blue Bump' emission is produced by an accretion disk surrounding the central black hole (e.g. Shields (1978); Malkan & Sargent (1982); Malkan (1983); Band & Malkan (1989)). The soft X-ray emission can be explained by Compton scattering of thermal UV photons in a layer of hot electrons above the disk (e.g. Czerny & Elvis (1987); Laor & Netzer (1989); Ross et al. (1992); Mannheim et al. (1995)). The closer to the Eddington limit the black hole accretes, the softer the X-ray spectrum is expected to become (e.g. Ross et al. (1992); Pounds et al. (1995)). Alternatively, the soft X-ray emission may also be result in an optically thick wind from the black hole region (King & Pounds (2003)).

In the days before ROSAT the study of strong soft X-ray AGN depended on serendipitous observations, e.g. by EINSTEIN (Córdova et al. (1992); Puchnarewicz et al. (1992)), and observations of AGN selected at optical wavelengths. Stephens (1989) noticed in a sample of EINSTEIN-selected AGN that more than 25% of her sources belonged to the Seyfert 1 (sub)class of Narrow-Line Seyfert galaxies (NLS1s, Osterbrock & Pogge (1985)), while in optically selected samples only about 10% of the sources are NLS1s (Osterbrock & Pogge (1985); Osterbrock (1987); Williams et al. (2003)) This higher fraction of NLS1s among X-ray selected sources was confirmed by Puchnarewicz et al. (1992) for a sample of 52 EINSTEIN-detected AGN: 9 of their 17 Seyfert 1 galaxies were NLS1s. Grupe (1996); Grupe et al. (1999b), and Edelson et al. (1999) found that in soft X-ray selected ROSAT AGN samples up to 40% were NLS1s. NLS1s show extreme properties, such as steep X-ray spectra (e.g. Boller et al. (1996); Grupe (1996); Williams et al. (2003)), strong optical FeII and weak emission from the Narrow-Line Region (e.g. Boroson & Green (1992); Boroson (2002); Grupe (1996);

Laor et al. (1997); Grupe et al. (1999b)).

We have studied the continuum and emission line properties of a sample of 76 soft X-ray selected ROSAT AGN (Grupe (1996); Grupe et al. (1998a, 1999b)). However, that sample was incomplete lacking a significant number of sources for which optical spectra were not obtained at that time. Our new sample containing 110 sources is complete following the criteria in §2. For each source X-ray and optical spectra exist that have enough quality to allow for a detailed analysis of their X-ray and optical properties. We performed a detailed study of the X-ray properties of the complete soft X-ray selected AGN sample (Grupe et al. (2001a)). Here we describe the sample selection (§2), the observations (§3), and data reduction (§4). The FeII subtraction and the line measurements are described in §5. We present an analysis of the distributions of continuum and emission line properties of NLS1s and BLS1s in §6. The results will be discussed in §7. Previously unpublished optical spectra are presented at the end of the paper. In a second paper (Grupe (2003), Paper II) we will present direct correlations and a Principal Component Analysis.

Throughout the paper spectral slopes are defined as energy spectral slopes with $F_\nu \propto \nu^{-\alpha}$. Luminosities are calculated assuming a Hubble constant of $H_0 = 75 \text{ km s}^{-1} \text{ Mpc}^{-1}$ and a deceleration parameter of $q_0 = 0.0$.

2. Sample Selection

Our AGN sample was selected from the bright soft X-ray sample presented by Thomas et al. (1998), using the following criteria:

- Mean RASS PSPC count rate $\geq 0.5 \text{ cts s}^{-1}$
- Hardness ratio³ < 0.00
- Galactic latitude $|b| > 20^\circ$

A count rate threshold of 0.5 was chosen to ensure sufficient X-ray photons during a typical RASS time coverage of about 200-400s to perform spectral analysis. The hardness ratio criterion ensures a soft X-ray spectrum and the galactic latitude criterion ensures no hardening of the X-ray

³Hardness ratio = (hard-soft)/(hard+soft) with the soft energies = 0.1-0.4 keV and hard energies = 0.5-2.0 keV.

spectrum due to extinction. Using these criteria, Thomas et al. (1998) found 397 sources of which 113 turned out to be AGN (Thomas et al. (1998); Grupe et al. (2001a)), excluding BL Lac objects that have different emission mechanisms. We have also excluded the three known transient sources from the present sample (IC 3599, Brandt et al. (1995); Grupe et al. (1995a); WPVS007, Grupe et al. (1995b), and RX J1624.9+7554, Grupe et al. (1999a)), because these sources were observed to be bright in X-rays only once and at least in IC 3599 and RX J1624.9+7554 the X-ray emission might be due to a dramatic accretion event (e.g. Gezari et al. (2003)). The nature of the X-ray transience in WPVS 007 is still unclear..

3. Observations

3.1. X-ray data

In addition to the RASS data, available for all sources, about 50 have pointed PSPC observations and are available from the ROSAT public archive at MPE Garching. A detailed description of the X-ray observations and analysis is given in Grupe et al. (2001a).

3.2. Optical spectroscopy

Optical spectroscopy data in the rest frame H β region were collected over a period of 10 years using various observatories and telescopes. Table 1 summarizes the observations. The table contains the coordinates of the X-ray position of the source in Equinox J2000, a common name, the observing date, the telescope and instrument, the observation time and comments. The comments list references to spectra that have been already published and weather conditions. In the following we describe the observations by telescope as they appear in Table 1.

3.2.1. ESO 2.2m and 1.52 m telescopes

All observations of objects with southern declination prior to 1995 were observed with the MPI/ESO 2.2m telescope at La Silla (ESO2.2 in Table 1). At that time, the 2.2m was equipped with the ESO Faint Object Camera and Spectrograph (EFOC), which had a selection of different grisms for spectroscopy. Table 1 lists the number of the grism(s) used. The grisms had the following

resolutions and wavelength coverages:

- #4: 2.2 Å/pix \approx 7 Å FWHM resolution, 4650 – 6800 Å
- #8: 1.3 Å/pix \approx 4 Å FWHM resolution, 4640 – 5950 Å
- #9: 1.1 Å/pix \approx 4 Å FWHM resolution, 5875 – 7020 Å
- #10: 1.2 Å/pix \approx 4 Å FWHM resolution, 6600 – 7820 Å

Slit widths were usually 1.''5 or 2.'' and the slit orientation was always in E-W direction.

The observations in 1995 and 1999 were performed with ESO's 1.52m telescope equipped with the Boller & Chivens spectrograph (B&C). At both times, the grating #23 with 600 grooves mm⁻¹ resulting in a dispersion in first order of 126 Å mm⁻¹ or 1.89 Å Pixel⁻¹. The resolution was about 6Å FWHM. For all the spectra we used a slit width of 2''.1. All observations with the ESO 1.52m telescope were performed at parallactic angle.

3.2.2. McDonald Observatory 2.1m and 2.7m telescopes

The telescope used for most northern hemisphere observations was the 2.1m Otto Struve telescope at McDonald Observatory. The ES2 spectrograph, which has a similar design to the Boller & Chivens spectrograph, used grating #22 during the 1994 run, giving a dispersion of 112Å mm⁻¹ (\approx 4Å FWHM resolution). During the 1995 to 1999 runs, grating #4 with 222Å mm⁻¹ (\approx 8Å FWHM resolution) was used. The slit widths for the 1995 to 1999 observing runs were either 1''.6 or 2''.0 and the slit orientation was in E-W direction for all observations.

A number of sources were observed with the Large Cassegrain Spectrograph (LCS) on the 2.7m Harlan-Smith Telescope at McDonald Observatory. Several of these sources are from an overlapping program of studies of PG quasars (Wills et al. (2000); Shang et al. (2003)). The slit width of the PG quasars was 1'' and 2'' for all other objects observed with the 2.7m telescope. The slit orientation was in E-W direction. The instrumental resolution was \approx 7Å(Shang et al. (2003)) for

the PG quasars and 14 for the other sources. One of the PG quasars, PG 1626+554, was observed with the Hubble Space Telescope (HST) using the Faint Object Spectrograph (FOS) with a $0.86''$ circular width.

3.2.3. CTIO and Tautenburg

A few objects were observed with the 4m Blanco telescope at the Cerro Tololo International Observatory in Chile (CTIO4.0 in Table 1). The instrument used was the R-C spectrograph with the KPGL3 grating having a dispersion of 116 \AA mm^{-1} (4.3 \AA FWHM resolution) with a slit width of $2''$. The slit was oriented in E-W direction.

Four sources were observed with the 2.0m telescope of the Thüringer Landessternwarte (TLS) Tautenburg, Germany, (TLS2.0 in Table 1) during the test stage of the Nasmyth Focal Reducer Spectrograph (NFRS) which was constructed and built at TLS. The V200 grism, with $300 \text{ grooves mm}^{-1}$ corresponding to a dispersion of 225 \AA mm^{-1} or 3.38 \AA px^{-1} , was used. The grism provides a wavelength coverage from 4500 to 9000 \AA . The slit width of $1''$ for B21128+31 and $2''$ for the other objects yields a resolution of 7 \AA or 14 \AA , respectively. Slit orientation was fixed (N-S direction).

4. Data reduction

All spectra, except for the ones taken at Tautenburg (see below), were bias and flat-field corrected and were wavelength- and flux-calibrated by taking spectra of calibration lamps and flux calibration standard stars. All data were reduced, except for the McDonald 2.7m and CTIO data, with ESO's MIDAS data reduction package. The McDonald 2.7m and CTIO data were reduced using IRAF. The 1D-spectra were extracted from the two-dimensional spectra using the optimal extraction algorithm as described by Horne (1986).

The data taken at TLS Tautenburg required special treatment because no calibration files were obtained. The bias was estimated from unexposed parts of the CCD. No flatfield correction was applied.

The TLS Tautenburg is located about 10 km north-east of the city of Jena. Usually, light pollution from cities can severely harm astronomical

observations. However, in our case the illumination of the sky by Jena's street lamps gave us a perfect night sky wavelength calibration spectrum. Osterbrock & Martel (1992) describe how the light pollution at Lick Observatory can be used for wavelength calibration. We identified the emission lines of the street lamps of Jena in the observed spectra and used these for the wavelength calibration.

The flux calibration was more challenging, because no standard star was observed. However, by chance a star was in the slit of three exposures at $\alpha_{2000} = 10\text{h } 40\text{m } 01.0\text{s}$, $\delta_{2000} = 21^{\circ} 08' 34''$. From the colors derived from the Automatic Plate Measuring (APM) scans of the Palomar Observatory Sky Survey plates (POSS) and 2 Micron All-Sky Survey (2MASS) we could identify the star as a K3V star. The known spectral shape of a K3V star allowed us to correct for the detector/telescope response and atmospheric transmission. The flux density was then determined from the APM magnitudes of the K3V star, using the K3V star RX J1320.7+0701 (Thomas et al. (1998)) as a reference.

Figure 1 shows the spectrum of RX J1304.2+0205 taken with the 2.7m at McDonald Observatory and the TLS Tautenburg. The figure demonstrates how well the calibration of the Tautenburg data matches the McDonald Observatory data.

5. Line measurements

5.1. FeII subtraction

In general, Seyfert 1 galaxies show FeII emission in their optical spectra. The strength of the FeII emission is correlated with the softness of the X-ray spectrum and anti-correlated with the strength of the [OIII] emission (e.g. Boroson & Green (1992); Boroson (2002); Grupe et al. (1999b)). In order to accurately measure the [OIII] and $H\beta$ emission lines, the FeII emission must be removed from the spectrum. This is especially important for sources with weak [OIII] emission, which are the ones with the strongest FeII emission.

We adopt the method described by Boroson & Green (1992), using the FeII template of IZw 1 given in their paper for the wavelength range $\sim 4400\text{-}6000 \text{ \AA}$. In order to correct also for the bluer part of the spectrum, this template was extended

towards shorter wavelengths using the relative FeII line intensities given by Phillips (1978a,b). The whole template was wavelength-shifted according to the redshift of the object's spectrum and the individual FeII lines were broadened to the FWHM of the broad H β line by using a Gaussian filter. The template was scaled by eye to match the line intensities of the object spectrum and then subtracted.

The FeII rest frame equivalent width and flux were measured in the rest frame range between 4430-4700Å (λ 4570Å blend) from the redshifted and scaled template. This wavelength range allows a direct comparison with the EW(FeII) given in Boroson & Green (1992). By measuring the FeII flux and equivalent width from the template instead of the source spectrum, we avoid contamination of the HeII λ 4686 line to the measurements. Note that the FeII/H β and EW(FeII) values given for the old sample (Grupe et al. (1999b)) were based on the flux in the entire template between 4250Å-5880Å.

The method of subtracting an FeII template of the NLS1 I Zw 1 from the AGN spectrum works well for most of the sources (e.g. RX J2242.6-3845 or MS 23409-1511). However, in some cases the FeII subtracted spectrum shows large residuals. Measurements of the FeII equivalent widths and fluxes from these sources have to be taken with caution. This is the case for the following objects: Mkn 335, Mkn 1044, RX J1005.7+4332, Mkn 141, Mkn 142, NGC 4051, QSO 1421-0013, and NGC 7214.

The reason for these discrepancies is that the template used was derived from one galaxy (I Zw 1) which is likely to have different physical conditions (temperature, electron density, ionization spectrum). The strengths of the different FeII atomic transitions depend strongly on these conditions (e.g. Sigut & Pradhan (2003) and Verner et al. (2003)). If the conditions in the BLR of our sources deviate from those in I Zw 1, we can expect that the template will not completely work to subtract and describe the FeII emission in this source.

5.2. Emission line and continuum parameters

Table 2 summarizes the redshifts, the FWHM, rest frame equivalent widths (EW), and the [OIII]/H β and FeII/H β line ratios measured from the optical spectra. The FWHM of the H β and [OIII] λ 5007 lines were measured directly from the lines. For the H β line, FWHM, EW and flux were measured in the broad component after subtracting a narrow component. This narrow component was constructed from an appropriately scaled template of the [OIII] λ 5007 line (Grupe et al. (1998b, 1999b)). All FWHM are given in the rest frame and are corrected for instrumental broadening assuming that $FWHM_{\text{true}} = \sqrt{FWHM_{\text{obs}}^2 - FWHM_{\text{instr}}^2}$. Due to the differing weather conditions for the observations, no line fluxes are given, only line ratios. Note that the [OIII]/H β line ratio is the flux of the [OIII] λ 5007 line to the broad component of H β and not the narrow component, as used in the diagrams of Veilleux & Osterbrock (1987).

Errors in the FWHM are typically $\approx 10\%$ for the H β line, but are larger for the [OIII] line due to the contamination of FeII and uncertainties in corrections for observational and instrumental resolution. The errors in the equivalent widths are critically dependent on determination of the continuum and can be as much as 25%, and in some cases where the FeII subtraction was less satisfactory they can be even larger. Another source of uncertainty in the equivalent width is in the contribution of star light from the host galaxy. This is more important for the low-luminosity than for the high-luminosity AGN. Additional errors of the H β FWHM and EW are the uncertainties of the subtraction of a narrow H β component. While it is quite easy to subtract a narrow H β component in Seyfert 1.5 galaxies, such as Mkn 1048, it is more complicated in NLS1s. Adjusting the [OIII] λ 5007 template by eye usually results in a [OIII]/H β_{narrow} ratio of about 3 while this ratio is typically 10-15 in Seyfert 1.5s (e.g. Cohen (1983)). We therefore measured the H β line twice, once with an [OIII]/H β_{narrow} ratio determined from the template adjusted by eye and second from a [OIII]/H β_{narrow} =10 ratio of the template. This was used to estimate the error in the H β FWHM and EW. The optical continuum and line luminosities for an individual source can be

in error by a factor of two to three due to non-photometric weather, bad seeing, and slit losses.

Table 3 lists the soft X-ray 0.2-2.0 keV spectral index α_X (Grupe et al. (2001a)), the rest frame 0.2-2.0 X-ray luminosity L_X , the optical monochromatic luminosity at 5100Å, λL_{5100} , the bolometric luminosity L_{bol} , and the soft X-ray short-term variability parameter χ^2/ν (Grupe et al. (2001a)). The bolometric luminosity was estimated from a combined powerlaw model fit with exponential cutoff to the optical-UV data and a powerlaw with absorption due to neutral elements, to the soft X-ray data (see Figure 2). Note that because the EUV part of the spectral energy distribution of AGN is unobservable, there are large uncertainties in the bolometric luminosity (e.g. Elvis et al. (1994)) and the values given here are only approximate.

6. Results

We classified all objects with $FWHM(H\beta) \leq 2000$ km s⁻¹ as Narrow Line Seyfert 1s (NLS1s) and all sources with $FWHM(H\beta) > 2000$ km s⁻¹ as Broad Line Seyfert 1s (BLS1s) following the definition of Osterbrock & Pogge (1985) and Goodrich (1989) regardless of subgroups such as Sy 1.5s. This results in 51 NLS1s and 59 BLS1s.

6.1. Simple Statistics

Table 4 summarizes the mean, standard deviations, medians of the FWHM of H β and [OIII], the rest frame equivalent widths of H β , [OIII] and FeII, the [OIII]/H β and FeII/H β flux ratios, the X-ray slopes α_X , the rest frame 0.2-2.0 keV X-ray luminosities, the 5100Å rest frame monochromatic luminosities, the bolometric luminosities, and the redshifts of the whole sample of 110 AGN, the 51 NLS1s, and the 59 BLS1s. NLS1s have in general the steepest X-ray spectra and strongest FeII emission, shown both in the equivalent width of FeII as well as in the FeII/H β line ratio. There are no differences between NLS1s and BLS1s with respect to their mean equivalent width of H β and luminosities in X-rays and at 5100Å. Kolmogorov-Smirnov KS tests for these properties show that the distributions are similar.

Figure 3 displays the distributions of the FWHM of H β and [OIII]. Due to their definition, they have different distributions of their FWHM(H β).

NLS1s and BLS1s have similar distribution in their FWHM([OIII]). Figure 4 shows the distributions of the equivalent widths of H β , [OIII], and FeII. There are no differences in the distributions of the EW(H β) (Figure 4a), but the EW(FeII) distributions (Figure 4c) are different at a level $P > 99.99\%$. NLS1s dominate the group with small values of the EW([OIII]). KS tests indicate that the EW([OIII]) distributions (Figure 4b) of NLS1s and BLS1s are only marginally different with a probability of 99.1%

Figure 5 displays the distributions of the X-ray spectral index in the ROSAT PSPC energy range. NLS1s have, as expected, the steepest X-ray spectra while BLS1s show flatter X-ray spectra. There is a $>99.99\%$ probability that the distributions are different.

The distributions in the rest frame 0.2-2.0 X-ray luminosities and the bolometric luminosities are shown in Figure 6. There are no significant differences in any of the luminosity distributions between NLS1s and BLS1s. Figure 7 displays the redshift distributions of the two samples. A KS-test shows that the distributions are similar.

Figure 8 displays the distributions of the [OIII] and FeII luminosities. A KS test shows that NLS1s and BLS1s have different distributions in their FeII luminosity ($P > 99.99\%$), but show similar distributions in their [OIII] luminosity. Figure 9 shows the distributions of the [OIII]/H β and FeII/H β flux ratios. While a KS test shows that the distributions of FeII/H β of NLS1s and BLS1s are clearly different, there is a 3% chance that the [OIII]/H β distributions are similar.

Figure 10 shows the distributions of the short-term variability parameter χ^2/ν of the RASS observations (Grupe et al. (2001a)). A KS test shows that the distributions are different with a probability of $P > 99.99\%$.

6.2. Spectra

Figure 11 displays all optical spectra in the observed frame that have not been published yet. For many of the sources, optical spectra are shown here for the first time. In other cases, spectra have been published before as listed in Table 1, but the spectra shown here are either of better quality or show a wider wavelength coverage. The spectra previously published by Grupe et al. (1999b) can

be accesses electronically at the CDS anonymous FTP site at *ftp 130.79.128.5*.

Figure 12 displays the FeII-subtracted spectra, the template used and the original spectra before template subtraction. The FeII subtracted spectra are shown with their calibrated fluxes. The FeII template and the original spectra are offset.

Please note: this is a special version for astro-ph that does not contain the optical and FeII subtracted spectra due to disk space limitations. The complete paper including the spectra can be retrieved from http://www.astronomy.ohio-state.edu/~dgrupe/research/sample_paper1.html

7. Discussion

7.1. Statistics

The main aims of this paper are to present the spectra and a simple statistical analysis of our sample of 110 soft X-ray selected AGN. About half of the sources of our complete sample of soft X-ray selected AGN turn out to be NLS1s (51). In a second paper (Grupe (2003)) a Principal Component Analysis (PCA) will be shown. The NLS1s show the well-known Boroson & Green (1992) Eigenvector 1 relation between [OIII] and FeII. It is not a complete surprise that about half of our sources are NLS1s, because NLS1s do have the steepest X-ray spectra among AGN (e.g. Boller et al. (1996); Grupe et al. (1999b, 2001a); Grupe (2000)) and the best way to find them is through a soft X-ray survey.

It is surprising that there is no significant difference between the rest frame 0.2-2.0 keV X-ray and 5100Å, and bolometric luminosities for NLS1s and BLS1s. Even though the sources are variable in X-rays (Grupe et al. (2001a)) the rest frame 0.2-2.0 keV X-ray luminosity is a better measure of power output of the nucleus than the optical luminosity here because of the different weather conditions, it is impossible to get absolute flux calibrated spectra if the conditions were not photometric. The other reason is that most of the spectra have been taken with 2'' slit widths, which means that the contribution of galactic starlight can be significant, especially for the low-luminosity AGN. The contribution to the total X-ray luminosity of sources such as high-luminous X-ray binaries of supernova remnants, is on the order of about $10^{31} - 10^{33}$ W, and is therefore negligible com-

pared with the X-ray power of the nucleus.

The usual interpretation of the steep X-ray spectra of NLS1s is that these sources accrete close to their Eddington limit (e.g. Pounds et al. (1995)). If this is true and the distributions in luminosity of all types of sources in our sample are the same we can interpret this result to imply that in general NLS1s have smaller central black hole masses than BLS1s as suggested by Boller et al. (1996) and Wandel & Boller (1998) and shown for some NLS1s by e.g. Onken et al. (2003). This assumption applies also for our sample. Grupe et al. (2003) found, that for the soft X-ray selected sample presented here, for a given luminosity, NLS1s have smaller black hole masses than BLS1s when the black hole masses were determined by the relations given in Kaspi et al. (2000). It will also be shown in that paper, that NLS1s show a different $M_{\text{BH}} - \sigma$ relation (Magorrian et al. (1998); Tremaine et al. (2003)) than non-active galaxies and broad-line Seyferts.

7.2. [OIII] and FeII strengths

There are two interesting things about the distributions of [OIII] and FeII strengths: a) for the luminosity distributions NLS1 and BLS1s have similar FeII luminosity distributions but different [OIII] luminosity distributions, and b) surprisingly the [OIII]/H β distributions are only slightly different with a 3% change of being similar, but the FeII/H β distributions are clearly different. From the Boroson & Green (1992) Eigenvector 1 relation, which we also see in our sample (Paper II), one would expect that also the FeII luminosity and [OIII]/H β distributions of NLS1s and BLS1s would be different. On the other hand, NLS1s and BLS1s do show slightly different distributions of their [OIII] equivalent widths and clearly different distributions of their FeII λ 4560 equivalent widths.

One has to keep in mind that due to the slit widths of about 2'', a contribution from circumnuclear HII regions cannot be excluded. The contribution of hydrogen absorption lines of a medium age stellar population can also be a problem. The typical contribution of this component is on the order of 2-3 Å in the equivalent widths of the Balmer lines (e.g. Shields & Searle (1978); McCall et al. (1985); Ho et al. (1997); Popescu & Hopp (2000); Meusinger & Brunzendorf (2002).

The $H\beta$ equivalent widths of the sources of our sample are much larger than this value (Tab 2 and 4) and the effect of stellar absorption lines can be neglected.

8. Conclusions

We have presented the optical data of a complete sample of 110 soft X-ray selected AGN. We found that

- About half of the sources are NLS1s based on their $\text{FWHM}(H\beta) \leq 2000 \text{ km s}^{-1}$.
- NLS1s and BLS1s show clearly different distributions of their α_X , rest frame equivalent widths of FeII, their FeII/ $H\beta$ ratios, FeII luminosities, and soft X-ray variability. KS tests also suggest slightly different distributions of $[\text{OIII}]/H\beta$ and $\text{EW}([\text{OIII}])$.
- NLS1s and BLS1s show similar distributions in their redshifts, continuum luminosities, and equivalent widths of $H\beta$
- The similar continuum luminosities in both sub-samples and the high accretion to mass ratios in NLS1s suggests that these have smaller black hole masses for a given luminosity than BLS1s.

Correlation analysis of the sample including a Principal Component Analysis will be presented in a second paper (Grupe (2003)). The black hole masses and their relation to the Magorrian et al. (1998) and Tremaine et al. (2003) $M_{\text{bh}} - \sigma$ relation will be presented in Grupe et al. (2003).

We would like to thank Marianne Vestergaard for comments and suggestions on the manuscript, the anonymous referee for a fast referee report that helped improving the paper, Hans-Christoph Thomas for providing the spectrum of the K3V star RX J13020.7+0701, and Brad Peterson for providing a spectrum of NGC 4593. We also want to thank the night assistants and technical people at La Silla and McDonald observatory, namely, Hector Vega, Dave Doss, Jerry Martin and Earl Green. Without their support this project would not have been possible. This research has made use of the NASA/IPAC Extra-galactic Database

(NED) which is operated by the Jet Propulsion Laboratory, Caltech, under contract with the National Aeronautics and Space Administration. The ROSAT project is supported by the Bundesministerium für Bildung und Forschung (BMBF/DLR) and the Max-Planck-Society.

REFERENCES

- Beuermann, K., Thomas, H.-C., Reinsch, K., et al., 1999, *A&A*, 347, 47
- Band, D.L., & Malkan, M.A., 1989, *ApJ*, 345, 122
- Boller, T., Brandt, W.N., & Fink, H.H., 1996, *A&A*, 305, 53
- Boroson, T.A., & Green, R.F., 1992, *ApJS*, 80, 109
- Boroson, T.A., 2002, *ApJ*, 565, 78
- Boroson, T.A., & Green, R.F., 1992, *ApJS*, 80, 109
- Brandt, W.N., Pounds, K.A., & Fink, H.H., 1995, *MNRAS*, 273, L47
- Cohen, R.D., 1983, *ApJ*, 273, 489
- Córdova, F.A., Kartje, J.F., Thompson, R.J., et al., *ApJS*, 81, 661
- Czerny, B., & Elvis, M., 1987, *ApJ*, 321, 305
- Dietrich, M., Kollatschny, W., Alloin, D., et al., 1994, *A&A*, 284, 33
- Edelson, R., Vaughan, S., Warwick, R., Puchnarewicz, E., & George, I., 1999, *MNRAS*, 307, 91
- Elvis, M., Fiore, F., Wilkes, B.J., & McDowell, J., 1994, *ApJ*, 422, 60
- Gezari, S., Halpern, J.P., Komossa, S., Grupe, D., & Leighly, K.M., 2003, *ApJ*, 592, 42
- Goodrich, R.W., 1989, *ApJ*, 342, 224
- Grupe, D., 1996, PhD Thesis, Universität Göttingen

- Grupe, D., 2000, *New Astronomy Reviews* Vol. 44, proceedings of the workshop on 'Observational and Theoretical Progress in the Study of Narrow-Line Seyfert 1 Galaxies, Eds Th. Boller, W.N. Brandt, K.M. Leighly, and M.J. Ward, p455
- Grupe, D., 2003, *AJ*, to be submitted (Paper II)
- Grupe, D., Beuermann, K., Mannheim, K., et al., 1995a, *A&A*, 299, L5
- Grupe, D., Beuermann, K., Mannheim, K., Thomas, H.-C., Fink, H.H., & de Martino, D., 1995b, *A&A*, 300, L21
- Grupe, D., Beuermann, K., Thomas, H.-C., & Fink, H.H., 1998a, *A&A*, 330, 25
- Grupe, D., Wills, B.J., Wills, D., Beuermann, K., 1998b, *A&A*, 333, 827
- Grupe, D., Thomas, H.-C., & Leighly, K.M., 1999a, *A&A*, 350, L31
- Grupe, D., Beuermann, K., Mannheim, K., & Thomas, H.-C., 1999b, *A&A*, 350, 805
- Grupe, D., Thomas, H.-C., & Beuermann, K., 2001a, *A&A*, 367, 470
- Grupe, D., Thomas, H.-C., Leighly, K.M., 2001b, *A&A*, 369, 450
- Grupe, D., Mathur, S., et al. 2003, *AJ*, in prep.
- Ho, L.C., Filippenko, A.V., & Sargent, W.L., 1997, *ApJS*, 112, 315
- Horne, K., 1986, *PASP*, 98, 609
- Kaspi, S., Smith, P.S., Netzer, H., Moaz, D., Jannuzi, B.T., & Givon, U., 2000, *ApJ*, 533, 631
- King, A.R., & Pounds, K.A., 2003, *MNRAS*, in press, astro-ph/0305541
- Laor, A., & Netzer, H., 1989, *MNRAS*, 238, 897
- Laor, A., Fiore, F., Elvis, M., Wilkes, B.J., & McDowell, J.C., 1997, *ApJ* 477, 93
- Magorrian, J., Tremaine, S., Richstone, D., Bender, R., Bower, G., et al., 1998, *AJ*, 115, 2285
- Malkan, M.A., & Sargent, W.L.W., 1982, *ApJ*, 254, 22
- Malkan, M.A., 1983, *ApJ*, 268, 582
- Mannheim, K., Schulte, M., & Rachen, J., 1995, *A&A*, 303, L41
- Mathur, S., 2000, *MNRAS*, 314, L17
- McCall, M.L., Rybski, P.M., & Shileds, G.A., 1985, *ApJS*, 57, 1
- Meusinger, H., & Brunzendorf, J., 2002, *A&A*, 390, 439
- Onken, C.A., Peterson, B.M., Dietrich, M., Robinson, A., & Salamanca, I.M., 2003, *ApJ*, 585, 121
- Osterbrock, D.E., & Pogge, R.W., 1985, *ApJ*, 297, 166
- Osterbrock, D.E., & Martel, A., 1992, *PASP*, 104, 76
- Osterbrock, D.E., 1987, *Lecture Notes in Physics* 307, Springer Verlag, Heidelberg, p1
- Pfeffermann, E., Briel, U.G., Hippmann, H., et al., 1987, *SPIE*, 733, 519
- Phillips, M.M., 1978a, *ApJ*, 226, 736
- Phillips, M.M., 1978b, *ApJS*, 38, 187
- Popescu, C.C., & Hopp, U., 2000, *A&AS*, 142, 247
- Pounds, K.A., Done, C., & Osborne, J., 1995, *MNRAS*, 277, L5
- Puchnarewicz, E.M., Mason, K.O., Córdova, F.A., et al., *MNRAS*, 256, 589
- Ross, R.R., Fabian, A.C., & Mineshige, S., 1992, *MNRAS*, 258, 189
- Schwobe, A.D., Hasinger, G., Lehmann, I., et al., *AN*, 321, 1
- Shang, Z., Wills, B.J., Robinson, E.L., Wills, D., Laor, A., Xie, B., & Yuan, J., 2003, *ApJ*, 586, 52
- Shields, G.A., 1978, *Nature*, 272, 706
- Shields, G.A., & Searle, L., 1978, *ApJ*, 222, 821
- Sigut, T.A.A., & Pradhan, A.K., 2003, *ApJS*, 145, 15
- Stephens, S., 1989, *AJ*, 97, 10

- Tanaka, Y., Inoue, H., & Holt, S.S., 1994, PASJ, 46, L37
- Thomas, H.-C., Beuermann, K., Reinsch, K., et al., 1998, A&A, 335, 467
- Tremaine, S., Gebhardt, K., Bender, R., et al., 2003, ApJ, 574, 740
- Trümper, J., 1982, Adv. Space Res., 4, 241
- Turner, T.J., George, I.M., Grupe, D., et al., 1999, ApJ, 510, 178
- Vaughan, S., Edelson, R., Warwick, R.S., Malkan, M.A., & Goad, M.R., 2001, MNRAS, 327, 673
- Veilleux, S & Osterbrock, D.E., 1987, ApJS, 63, 295
- Verner, E., Bruhweiler, F., Verner, D., Johansson, S., & Gull, T., 2003, ApJ, 592, L59
- Voges, W., Aschenbach, B., Boller, T., et al., 1999, A&A, 349, 389
- Wandel, A., & Boller, T., 1998, A&A, 331, 884
- Williams, R.J., Pogge, R.W., & Mathur, S., 2003, AJ, 124, 3042
- Wills, B.J., Wills, D., Evans, N.J., Natta, A., Thompson, K.L., Breger, M., & Sitko, M.L., 1992, ApJ, 400, 96
- Wills, B.J., Netzer, H., & Wills, D., 1985, ApJ, 288, 94
- Wills, B.J., Shang, Z., & Yuan, J.M., 2000, New Astronomy Reviews Vol. 44, proceedings of the workshop on 'Observational and Theoretical Progress in the Study of Narrow-Line Seyfert 1 Galaxies, Eds Th. Boller, W.N. Brandt, K.M. Leighly, and M.J. Ward, p511

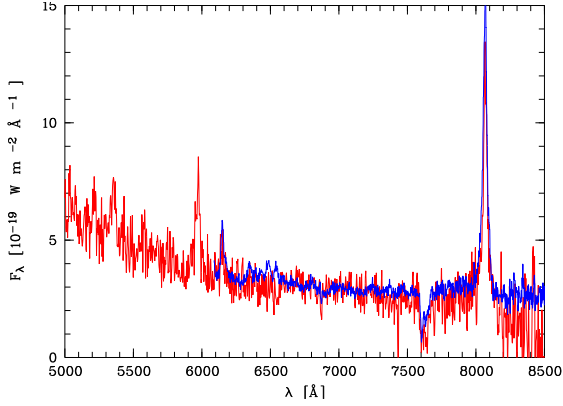


Fig. 1.— Combined spectrum of spectra of RX J1304.2+0205 taken at McDonald Observatory (black) and the Thüringer Landessternwarte Tautenburg (grey)

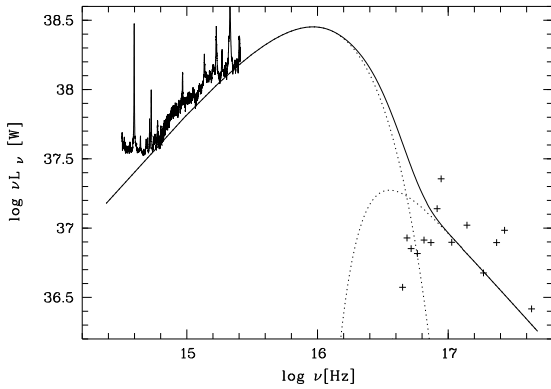


Fig. 2.— Powerlaw with exponential cutoff and powerlaw with neutral absorption (solid line) to the optical/UV (Shang et al. (2003)) and X-ray spectrum of PG 1115+407 as an example how the bolometric luminosity was determined. The dotted lines display the powerlaw with exponential cutoff for the optical/UV part and the powerlaw with neutral absorption for the soft X-ray part separately.

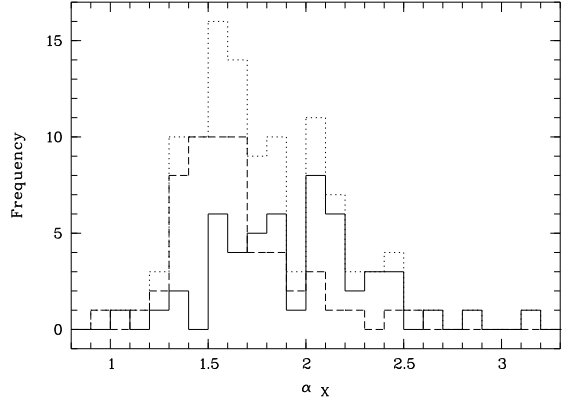


Fig. 5.— Distribution of the X-ray spectral slope α_X . The lines are the same as described in Figure 3.

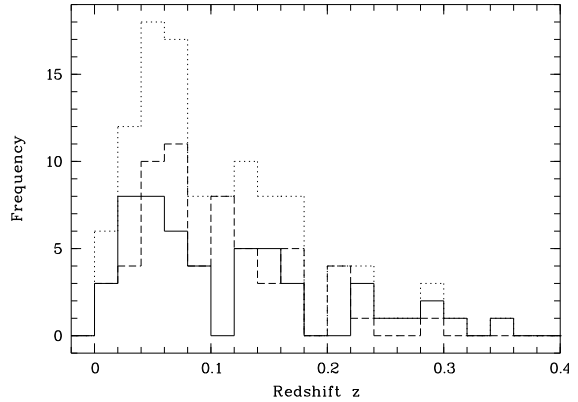


Fig. 7.— Distribution of the redshift z . The lines are the same as described in Figure 3.

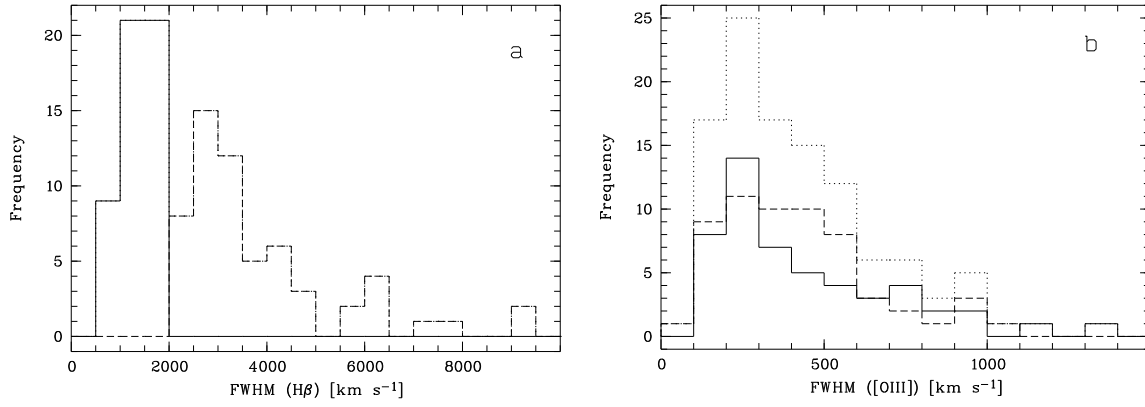


Fig. 3.— Distribution of the FWHM of $H\beta$ and $[OIII]$ for the whole sample (dotted line), NLS1s (solid line), and BLS1s (short dashed line). FWHM have been corrected for instrumental resolution.

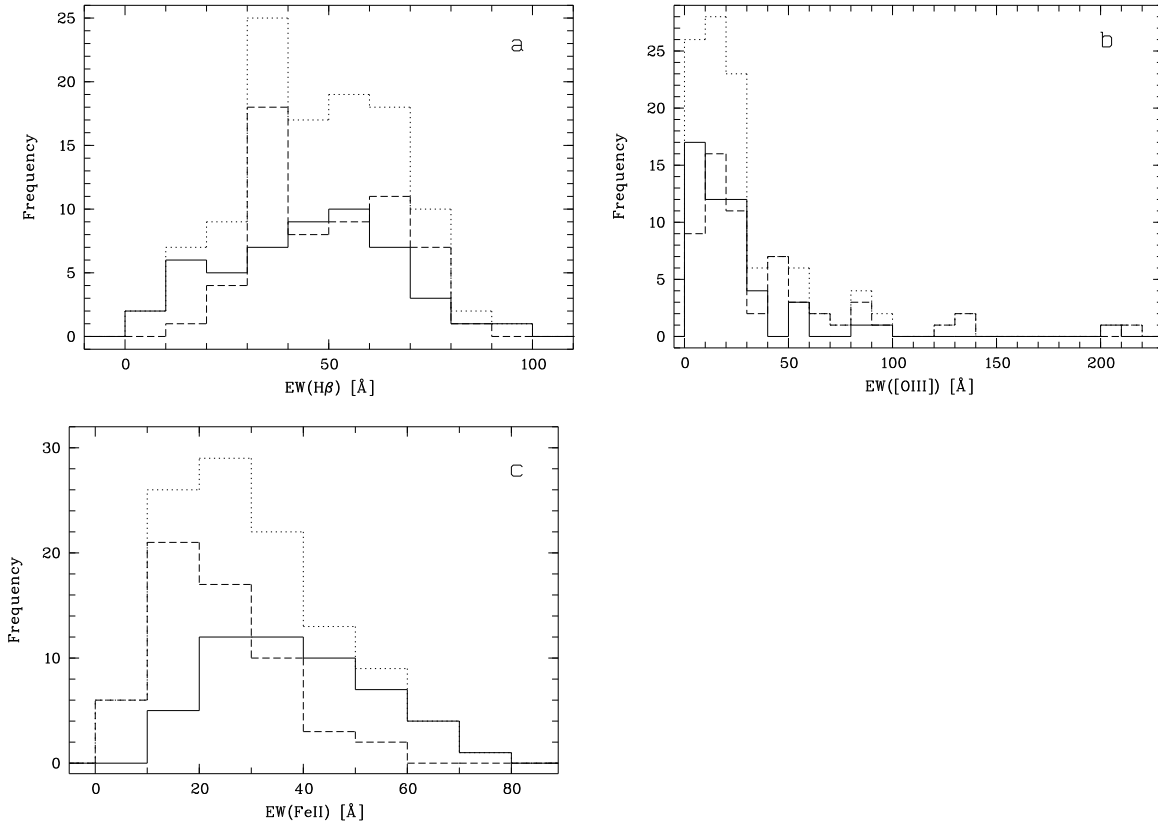


Fig. 4.— Distribution of the rest frame Equivalent widths of $H\beta$, $[OIII]$, and $FeII$. The lines are the same as described in Figure 3.

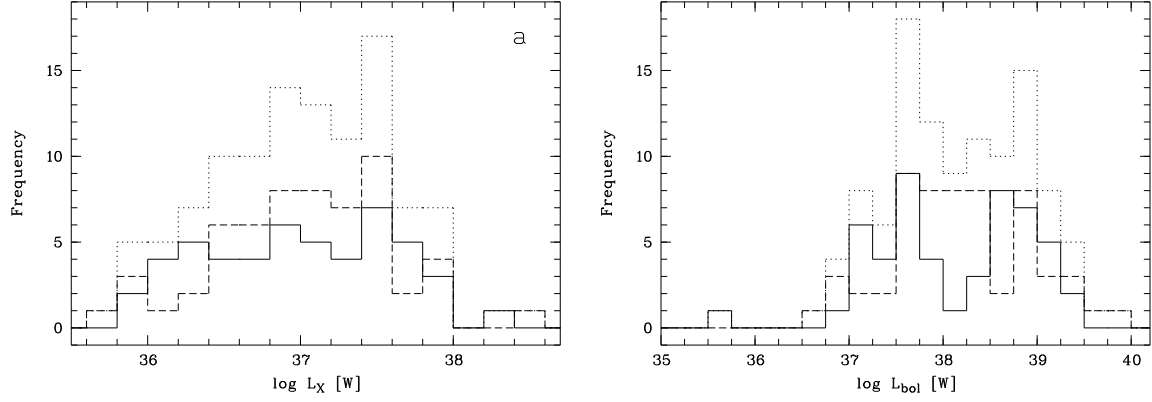


Fig. 6.— Distribution of the rest frame 0.2-2.0 keV X-ray luminosity L_X and the bolometric luminosity L_{bol} . The lines are as described in Figure 3.

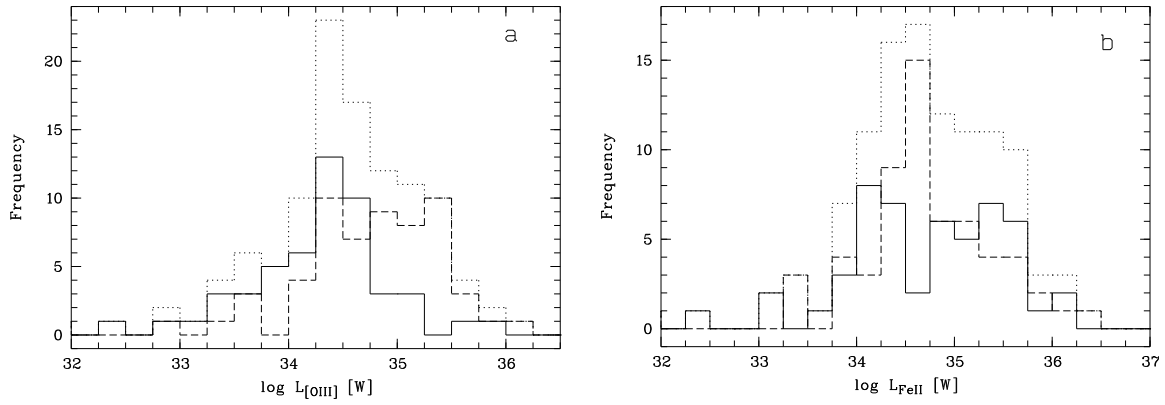


Fig. 8.— Distribution of the [OIII] (left) and FeII luminosities (right). The lines are the same as described in Figure 3.

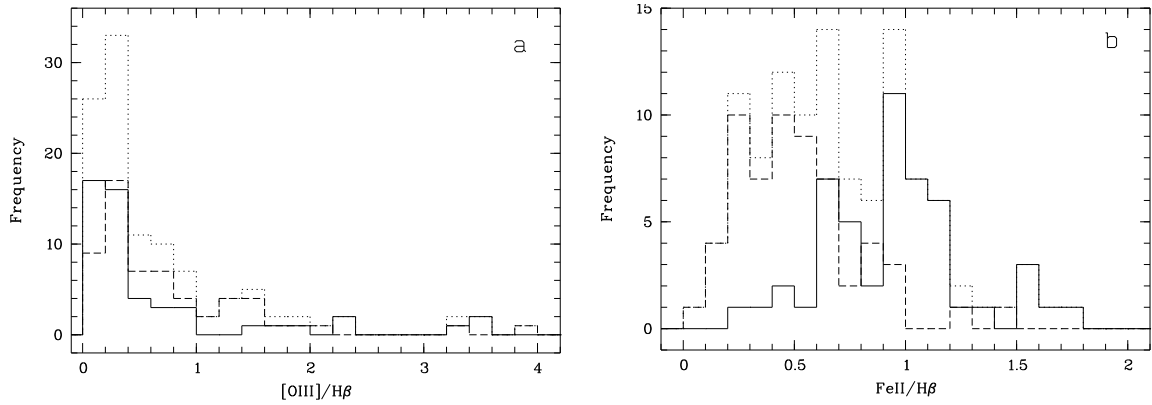


Fig. 9.— Distribution of the [OIII]/ $H\beta$ and FeII/ $H\beta$ flux ratios. The lines are the same as described in Figure 3.

TABLE 1
SUMMARY OF THE OPTICAL SPECTROSCOPY OF THE SOFT X-RAY SELECTED SAMPLE

No.	α_{2000}	δ_{2000}	Name	UT date	Tel.	Instrument	T_{exp}	comments
1	00 06 19.5	+20 12 11	Mkn 335	1999/09/13	ESO1.52	B&C	30	
2	00 25 00.2	-45 29 34	ESO 242-G8	1993/09/14	ESO2.2	EFOSC 1,8,10	5,30,30	Grupe et al. (1999b)
3	00 57 20.2	-22 22 57	Ton S 180	1992/10/17	ESO2.2	EFOSC 1,8,10	5,30,30	Grupe et al. (1999b)
4	00 58 37.4	-36.06.05	QSO 0056-36	1993/10/12	ESO2.2	EFOSC 1,8,10	10,25,20	Grupe et al. (1999b)
5	01 00 27.1	-51 13 54	RX J0100.4-5113	1993/10/12	ESO2.2	EFOSC 1,8,10	10,40,35	Grupe et al. (1999b)
6	01 05 38.8	-14 16 14	RX J0105.6-1416	1999/09/12	ESO1.52	B&C	30	light clouds, 2-3'' seeing
7	01 17 30.6	-38 26 30	RX J0117.5-3826	1999/09/14	ESO1.52	B&C	40	
8	01 19 35.7	-28 21 32	MS 0117-28	1995/10/01	ESO1.52	B&C	30	
9	01 28 06.7	-18 48 31	RX J0128.1-1848	1999/09/12	ESO1.52	B&C	30	seeing 2-3''
10	01 29 10.7	-21 41 57	IRAS F01267-217	1993/12/18	ESO2.2	EFOSC 1,8,10	5,30,20	Grupe et al. (1999b)
11	01 48 22.3	-27 58 26	RX J0148.3-2758	1992/08/26	ESO2.2	EFOSC 8,10	15,15	Grupe et al. (1999b)
12	01 52 27.1	-23 19 54	RX J0152.4-2319	1993/09/12	ESO2.2	EFOSC 1,8,10	5,30,30	Grupe et al. (1999b)
13	02 30 05.5	-08 59 53	Mkn 1044	1999/09/13	ESO1.52	B&C	30	
14	02 34 37.8	-08 47 16	Mkn 1048	1999/09/13	ESO1.52	B&C	30	light cirrus, seeing 2.2''
15	03 11 18.8	-20 46 19	RX J0311.3-2046	1999/09/13	ESO1.52	B&C	45	
16	03 19 48.7	-26 27 12	RX J0319.8-2627	1992/10/18	ESO2.2	EFOSC 1,8,10	5,30,30	Grupe et al. (1999b)
17	03 23 15.8	-49 31 11	RX J0323.2-4931	1993/08/21	ESO2.2	EFOSC 1,8,10	30,30,30	Grupe et al. (1999b)
18	03 25 02.2	-41 54 18	ESO 301-G13	1993/09/13	ESO2.2	EFOSC 1,8,10	5,45,45	Grupe et al. (1999b)
19	03 33 40.2	-37 06 55	VCV 0331-37	1993/09/14	ESO2.2	EFOSC 1,8,10	5,30,30	Grupe et al. (1999b)
20	03 49 07.7	-47 11 04	RX J0349.1-4711	1993/10/11	ESO2.2	EFOSC 1,9	10,40	Grupe et al. (1999b)
21	03 51 41.7	-40 28 00	Fairall 1116	1993/10/12	ESO2.2	EFOSC 1,8,10	5,30,20	Grupe et al. (1999b)
22	04 05 01.7	-37 11 15	ESO 359-G19	1999/09/12	ESO1.52	B&C	45	
23	04 12 41.5	-47 12 46	RX J0412.7-4712	1993/10/19	ESO2.2	EFOSC 1,8,10	5,30,30	Grupe et al. (1999b)
24	04 26 00.7	-57 12 02	1H 0419-577	1993/09/14	ESO2.2	EFOSC 1,8,10	5,20,15	Turner et al. (1999)
25	04 30 40.0	-53 36 56	Fairall 303	1993/10/10	ESO2.2	EFOSC 1,8,10	5,30,20	Grupe et al. (1999b)
26	04 37 28.2	-47 11 30	RX J0437.4-4711	1992/08/26	ESO2.2	EFOSC 8,10	15,15	Grupe et al. (1999b)
27	04 39 38.7	-53 11 31	RX J0439.6-5311	1999/09/14	ESO1.52	B&C	45	
28	04 41 22.5	-27 08 20	H 0439-272	1999/09/13	ESO1.52	B&C	30	
29	06 15 49.6	-58 26 06	1 ES 0614-584	1999/09/12	ESO1.52	B&C	30	
30	08 59 02.9	+48 46 09	RX J0859.0+4846	1998/03/04	McD2.1	ES2 G4	2x45	
31	09 02 33.6	-07 00 04	RX J0902.5-0700	1999/03/20	McD2.1	ES2 G4	45	
32	09 25 13.0	+52 17 12	Mkn 110	1995/03/07	McD2.1	ES2 G4	20	
33	09 56 52.4	+41 15 22	PG 0953+414	1996/05/13	McD2.7	LCS	35	Wills et al. (2000)
34	10 05 41.9	+43 32 41	RX J1005.7+4332	1995/04/02	McD2.1	ES2 G4	50	light clouds
35	10 07 10.2	+22 03 02	RX J1007.1+2203	1998/02/21	McD2.1	ES2 G4	60	
36	10 13 03.2	+35 51 24	CBS 126	1995/03 ¹	McD2.1	ES2 G4	160 ¹	¹
37	10 19 00.5	+37 52 41	HS1019+37	1999/03/13	McD2.7	LCS	45	
38	10 19 12.6	+63 58 03	Mkn 141	1995/03 ²	McD2.1	ES2 G4	110 ²	²
39	10 25 31.3	+51 40 35	Mkn 142	1995/03 ³	McD2.1	ES2 G4	190 ³	³
40	10 34 38.6	+39 38 28	RX J1034.6+3938	1998/03/04	McD2.1	ES2 G4	45	
41	11 17 10.1	+65 22 07	RX J1117.1+6522	1995/03 ⁴	McD2.1	ES2 G4	280 ⁴	⁴
42	11 18 30.4	+40 25 55	PG 1115+407	1997/02/13	McD2.7	LCS	45	Wills et al. (2000)
43	11 19 08.7	+21 19 18	Ton 1388	1995/03 ⁵	McD2.1	ES2 G4	155 ⁵	⁵
44	11 31 04.8	+68 51 53	EXO 1128+69	1998/03/04	McD2.1	ES2 G4	45	seeing 2.5''
45	11 31 09.5	+31 14 06	B2 1128+31	2002/02/14	TLS2.0	NFRS V200	4x15	seeing > 3''
46	11 38 49.6	+57 42 44	SBS 1136+579	1999/03/21	McD2.1	ES2 G4	60	
47	11 39 13.9	+33 55 51	Z 1136+3412	1999/03/20	McD2.1	ES2 G4	45	
48	11 41 16.2	+21 56 21	Was 26	1998/02/20	McD2.1	ES2 G4	45	clouds
49	11 44 29.9	+36 53 09	CASG 855	1998/02/21	McD2.1	ES2 G4	45	
50	12 01 14.4	-03 40 41	Mkn 1310	1998/03/04	McD2.1	ES2 G4	45	seeing 2.5''
51	12 03 09.5	+44 31 50	NGC 4051	1999/03/13	McD2.7	LCS	15	
52	12 04 42.1	+27 54 12	GQ Com	1996/04/17	McD2.7	LCS	40	Shang et al. (2003)
53	12 09 45.2	+32 17 02	RX J1209.8+3217	1999/03/14	McD2.7	LCS	45	
54	12 14 17.7	+14 03 13	PG 1211+143	1997/03/15	McD2.1	ES2 G4	20	clouds
55	12 18 26.6	+29 48 46	Mkn 766	1997/03/12	McD2.1	ES2 G4	30	clouds, Grupe et al. (1998b)
56	12 29 06.7	+02 03 09	3C 273	1996/02/15	McD2.7	LCS	10	Shang et al. (2003)
57	12 31 36.6	+70 44 14	RX J1231.6+7044	1999/03/22	McD2.1	ES2 G4	2x30	some clouds
58	12 32 03.6	+20 09 30	Mkn 771	1998/02/21	McD2.1	ES2 G4	45	seeing > 3''
59	12 33 41.7	+31 01 03	CBS 150	1999/03/22	McD2.1	ES2 G4	2x30	light clouds
60	12 36 51.2	+45 39 05	MCG+08-23-067	1999/03/20	McD2.1	ES2 G4	45	
61	12 39 39.4	-05 20 39	NGC 4593	1989/12/31	OSU 1.8	CCDS	40	Dietrich et al. (1994)
62	12 42 10.6	+33 17 03	IRAS F12397+3333	1997/03/12	McD2.1	ES2 G4	2x45	clouds, Grupe et al. (1998b)
63	12 46 35.2	+02 22 09	PG 1244+026	1998/03/04	McD2.1	ES2 G4	45	seeing > 3''
64	13 04 17.0	+02 05 37	RX J1304.2+0205	2002/02/14	TLS2.0	NFRS V200	4x15	
65	13 09 47.0	+08 19 48	PG 1307+085	1999/03/21	McD2.1	ES2 G4	30	

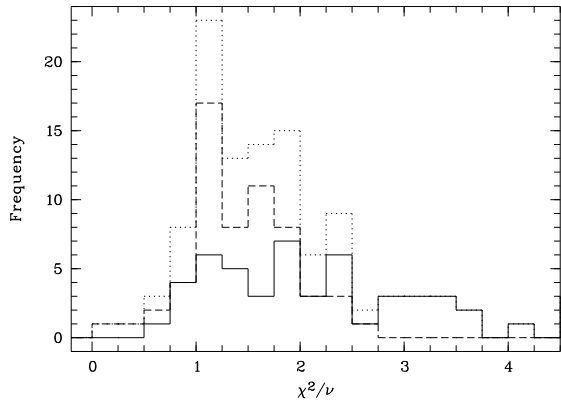


Fig. 10.— Distribution of the X-ray variability parameter χ^2/ν . Outside the plot are NGC 4051, Mkn 766, and RX J1304.2+0205 with $\chi^2/\nu=18.3$, 8.86, and 5.08, respectively. The lines are the same as described in Figure 3.

TABLE 1—*Continued*

No.	α_{2000}	δ_{2000}	Name	UT date	Tel.	Instrument	T_{exp}	comments
66	13 14 22.7	+34 29 39	RX J1314.3+3429	1995/03 ⁶	McD2.1	ES2 G4	310 ⁶	⁶
67	13 19 57.1	+52 35 33	RX J1319.9+5235	1999/03/13	McD2.7	LCS	45	
68	13 23 49.5	+65 41 48	PG 1322+659	1996/04/18	McD2.7	LCS	40	Shang et al. (2003)
69	13 37 18.7	+24 23 03	IRAS 13349+2438	1987/03/31	McD2.7	IDS ⁷	N/A	Wills et al. (1992)
70	13 43 56.7	+25 38 48	Ton 730	1999/03/20	McD2.1	ES2 G4	45	
71	13 55 16.6	+56 12 45	RX J1355.2+5612	1995/04/01	McD2.1	ES2 G4	45	
72	14 05 16.2	+25 55 34	PG 1402+261	1996/05/10	McD2.7	LCS	35	Wills et al. (2000)
73	14 13 36.7	+70 29 50	RX J1413.6+7029	1994/03/06	McD2.1	ES2 G22	35	Grupe et al. (1999b)
74	14 17 59.5	+25 08 12	NGC 5548	1995/02/25	McD2.1	ES2 G4	20	
75	14 24 03.8	-00 26 58	QSO 1421-0013	2002/02/14	TLS2.0	NFRS V200	4×15	
76	14 27 25.0	+19 49 53	Mkn 813	1999/03/21	McD2.1	ES2 G4	30	
77	14 31 04.1	+28 17 14	Mkn 684	1995/03 ⁸	McD2.1	ES2 G4	150 ⁸	
78	14 42 07.5	+35 26 23	Mkn 478	1995/03 ⁹	McD2.1	ES2 G4	150 ⁹	⁹
79	14 51 08.8	+27 09 27	PG 1448+273	2002/02/14	TLS2.0	NFRS V200	2×10	
80	15 04 01.2	+10 26 16	Mkn 841	1999/03/19	McD2.1	ES2 G4	30	
81	15 29 07.5	+56 16 07	SBS 1527+564	1998/03/04	McD2.1	ES2 G4	45	seeing \approx 3''
82	15 59 09.7	+35 01 48	Mkn 493	1997/03/14	McD2.1	ES2 G4	30	clouds
83	16 13 57.2	+65 43 11	Mkn 876	1995/04/01	McD2.1	ES2 G4	25	
84	16 18 09.4	+36 19 58	RX J1618.1+3619	1999/03/22	McD2.1	ES2 G4	45	clouds
85	16 19 51.3	+40 58 48	KUG 1618+40	1999/03/20	McD2.1	ES2 G4	50	
86	16 27 56.1	+55 22 32	PG 1626+554	1996/11/18	HST	FOS	4.25	Shang et al. (2003)
87	16 29 01.3	+40 08 00	EXO 1627+4014	1999/03/14	McD2.7	LCS	30	
88	17 02 31.1	+32 47 20	RX J1702.5+3247	1999/03/21	McD2.1	ES2 G4	2×30	
89	21 32 27.9	+10 08 20	II Zw 136	1999/09/13	ESO1.52	B&C G23	30	
90	21 46 36.0	-30 51 41	RX J2146.6-3051	1999/09/14	ESO1.52	B&C G23	30	light clouds
91	22 07 45.0	-32 35 01	ESO 404-G029	1999/09/13	ESO1.52	B&C G23	45	
92	22 09 07.6	-27 48 36	NGC 7214	1999/09/14	ESO1.52	B&C G23	20	light cirrus
93	22 16 53.2	-44 51 57	RX J2216.8-4451	1995/09 ¹⁰	ESO1.52	B&C G23	265 ¹⁰	
94	22 17 56.6	-59 41 30	RX J2217.9-5941	1995/09/21	ESO1.52	B&C G23	40	
95	22 30 40.3	-39 42 52	PKS 2227-399	1999/09/14	ESO1.52	B&C G23	2×40	light cirrus
96	22 42 37.7	-38 45 16	RX J2242.6-3845	1995/09 ¹¹	ESO1.52	B&C G23	300 ¹¹	¹¹
97	22 45 20.3	-46 52 12	RX J2245.2-4652	1995/09/28	ESO1.52	B&C G23	30	light clouds
98	22 48 41.2	-51 09 53	RX J2248.6-5109	1992/10/19	ESO2.2	EFOSC 1,8,10	5,30,30	Grupe et al. (1999b)
99	22 57 39.0	-36 56 07	MS 2254-36	1995/09 ¹²	ESO1.52	B&C G23	85 ¹²	¹²
100	22 58 45.4	-26 09 14	RX J2258.7-2609	1992/08/26	ESO2.2	EFOSC 1,8,10	5,20,20	Grupe et al. (1999b)
101	23 01 36.2	-59 13 20	RX J2301.6-5913	1999/06/19	CTIO4.0	R-C spec	10	
102	23 01 52.0	-55 08 31	RX J2301.8-5508	1995/09 ¹³	ESO1.52	B&C G23	255 ¹³	¹³
103	23 04 37.3	-35 01 13	RX J2304.6-3501	1992/08/25	ESO2.2	EFOSC 1,8,10	15,30,30	Grupe et al. (1999b)
104	23 12 34.8	-34 04 20	RX J2312.5-3404	1999/09/13	ESO1.52	B&C G23	2×30	
105	23 17 49.9	-44 22 28	RX J2317.8-4422	1995/09/19	ESO1.52	B&C G23	50	
106	23 25 11.8	-32 36 35	RX J2325.2-3236	1993/10/14	ESO2.2	EFOSC 1,4	5,30	Grupe et al. (1999b)
107	23 25 24.2	-38 26 49	IRAS 23226-3843	1999/06/21	CTIO4.0	R-C spec	10	clouds
108	23 43 28.6	-14 55 30	MS 23409-1511	1995/09	ESO1.52	B&C G23	3×40	
109	23 49 24.1	-31 26 03	RX J2349.4-3126	1992/08/21	ESO2.2	EFOSC 1,8,10	30,30,30	Grupe et al. (1999b)
110	23 57 28.0	-30 27 40	AM 2354-304	1999/09/12	ESO1.52	B&C G23	45	seeing \approx 3''

¹Mean of four spectra observed for a total of 160 min under different weather conditions²Mean of three spectra observed for a total of 110 min under different weather conditions³Mean of six spectra observed for a total of 190 min under different weather conditions⁴Mean of five spectra observed for a total of 280 min under different weather conditions⁵Mean of six spectra observed for a total of 155 min under different weather conditions⁶Mean of seven spectra for a total observing time of 310 min under different weather conditions.⁷IDS: Image Dissector Scanner; Wills et al. (1985)⁸Mean of five spectra with a total observing time of 150 min.⁹Mean of six spectra observed for a total of 150 min under different weather conditions¹⁰Mean of six spectra observed for a total of 265 min.¹¹Mean of five spectra observed for 60 min each under different weather conditions¹²Mean of three spectra observed for a total of 85 min under different weather conditions.¹³Mean of seven spectra observed for a total of 255 min under different weather conditions.

TABLE 2
LINE MEASUREMENTS OF THE SOFT X-RAY AGN SAMPLE

No.	Name	z	FWHM		Equivalent width		FeII	$\frac{[\text{OIII}]}{\text{H}\beta}$	$\frac{\text{FeII}}{\text{H}\beta}$			
			H β	[OIII]	H β	[OIII]						
1	Mkn 335	0.026	1710	± 140	425	± 65	72	± 10	25	50	0.33	0.62
2	ESO 242-G008	0.059	3000	± 200	320	± 50	59	± 5	52	24	0.87	0.43
3	Ton S 180	0.062	970	± 100	630	± 60	37	± 8	4	30	0.10	0.90
4	QSO 0056-36	0.165	4550	± 250	360	± 50	45	± 5	3	20	0.06	0.49
5	RX J0100.4-5113	0.062	3190	± 630	550	± 50	36	± 10	15	35	0.36	0.97
6	RX J0105.6-1416	0.070	2600	± 300	420	± 60	56	± 5	70	12	1.21	0.22
7	RX J0117.5-3826	0.225	900	± 100	420	± 50	50	± 10	8	32	0.15	0.72
8	MS 0117-28	0.349	1681	± 260	970	± 250	48	± 2	4	40	0.07	0.86
9	RX J0128.1-1848	0.046	2620	± 100	400	± 60	38	± 10	83	33	2.18	0.89
10	IRAS F01267-217	0.093	2520	± 160	360	± 50	60	± 2	23	33	0.32	0.60
11	RX J0148.3-2758	0.121	1030	± 100	700	± 500	82	± 2	5	51	0.05	0.69
12	RX J0152.4-2319	0.113	2890	± 250	615	± 50	57	± 10	33	37	0.54	0.68
13	Mkn 1044	0.017	1310	± 100	440	± 100	57	± 2	7	40	0.12	0.77
14	Mkn 1048	0.042	5670	± 160	435	± 60	68	± 2	48	15	0.63	0.23
15	RX J0311.3-2046	0.070	4360	± 680	640	± 75	40	± 2	15	11	0.35	0.29
16	RX J0319.8-2627	0.079	3100	± 1000	420	± 100	48	± 4	19	41	0.37	0.92
17	RX J0323.2-4931	0.071	1680	± 250	260	± 50	62	± 3	16	37	0.22	0.65
18	ESO 301-G013	0.059	2410	± 680	530	± 50	73	± 10	121	36	1.49	0.50
19	VCV 0331-373	0.064	1880	± 110	210	± 50	57	± 6	22	36	0.31	0.61
20	RX J0349.1-4711	0.299	1700	± 530	700	± 50	52	± 20	38	67	0.43	1.16
21	Fairall 1116	0.059	4310	± 630	340	± 50	67	± 5	18	22	0.24	0.34
22	ESO 359-G019	0.055	9430	± 760	405	± 60	78	± 10	27	6	0.40	0.08
23	RX J0412.7-4712	0.132	3520	± 940	140	± 50	42	± 4	41	5	0.89	0.12
24	1H 0419-577	0.104	2580	± 200	500	± 50	51	± 2	82	5	1.42	0.10
25	Fairall 303	0.040	1450	± 120	140	± 50	100	± 10	35	61	0.30	0.64
26	RX J0437.4-4711	0.052	3990	± 500	230	± 50	41	± 2	11	23	0.23	0.55
27	RX J0439.6-5311	0.243	700	± 140	1380	± 360	8	± 2	4	21	0.47	2.66
28	H 0439-272	0.084	2550	± 150	340	± 70	47	± 2	88	12	1.93	0.25
29	1 ES 0614-584	0.057	1080	± 100	200	± 50	29	± 5	4	27	0.13	1.00
30	RX J0859.0+4846	0.083	2990	± 150	130	± 130	74	± 3	42	24	0.50	0.31
31	RX J0902.5-0700	0.089	1860	± 150	230	± 130	73	± 10	21	45	0.27	0.68
32	Mkn 110	0.035	1760	± 50	170	± 140	65	± 7	52	18	0.71	0.26
33	PG 0953+414	0.234	3000	± 220	520	± 70	59	± 2	14	28	0.22	0.51
34	RXJ1005.7+4332	0.178	2740	± 250	950	± 100	36	± 2	2	44	0.07	1.41
35	RX J1007.1+2203	0.083	1460	± 270	170	± 130	42	± 20	16	30	0.27	0.69
36	CBS 126	0.079	2980	± 200	460	± 70	57	± 4	18	16	0.29	0.30
37	HS 1019+37	0.135	6200	± 2000	800	± 100	30	± 4	18	11	0.64	0.35
38	Mkn 141	0.042	3600	± 110	450	± 70	34	± 2	15	22	0.40	0.70
39	Mkn 142	0.045	1620	± 120	260	± 120	48	± 1	8	35	0.16	0.78
40	RX J1034.6+3938	0.044	700	± 110	340	± 100	12	± 2	24	18	1.65	1.37
41	RX J1117.1+6522	0.147	1650	± 170	1000	± 150	56	± 1	10	48	0.18	0.99
42	PG 1115+407	0.154	1740	± 180	340	± 100	53	± 8	6	49	0.10	0.98
43	Ton 1388	0.177	2770	± 140	950	± 110	73	± 3	8	46	0.10	0.72
44	EXO 1128+69	0.045	2130	± 150	200	± 140	28	± 15	25	15	0.84	0.55
45	B2 1128+31	0.289	3400	± 200	570	± 50	27	± 10	14	16	0.39	0.59
46	SBS 1136+579	0.116	2600	± 1000	400	± 100	30	± 6	23	25	0.70	0.86
47	Z 1136+3412	0.033	1450	± 125	190	± 130	41	± 20	16	43	0.30	1.02
48	Was 26	0.063	2200	± 440	220	± 150	37	± 5	136	21	3.84	0.60
49	CASG 855	0.040	4040	± 1000	200	± 140	18	± 10	27	13	1.25	0.61
50	Mkn 1310	0.019	3000	± 800	150	± 130	37	± 3	45	23	1.28	0.62
51	NGC 4051	0.002	1170	± 100	370	± 125	29	± 3	29	27	0.92	0.94
52	GQ Com	0.165	3870	± 350	290	± 110	38	± 6	50	19	1.19	0.45
53	RX J1209.8+3217	0.145	1320	± 110	820	± 100	58	± 4	34	58	0.56	1.09
54	PG 1211+143	0.082	1900	± 150	280	± 130	70	± 1	12	32	0.14	0.50
55	Mkn 766	0.013	1100	± 200	270	± 120	14	± 2	52	22	3.58	1.56
56	3C 273	0.158	3050	± 200	970	± 130	41	± 1	5	23	0.12	0.57
57	RX J1231.6+7044	0.208	4260	± 1250	540	± 60	35	± 10	70	19	1.56	0.37
58	Mkn 771	0.064	3200	± 100	210	± 150	73	± 2	21	28	0.28	0.42
59	CBS 150	0.290	1350	± 100	460	± 50	47	± 3	15	38	0.25	0.82
60	MCG+08-23-067	0.030	730	± 140	600	± 60	9	± 3	24	10	2.38	1.08
61	NGC 4593	0.009	4910	± 300	180	± 150	25	± 1	17	11	0.66	0.43
62	IRAS F12397+3333	0.044	1640	± 250	510	± 100	26	± 10	53	44	1.85	1.79
63	PG 1244+026	0.049	830	± 50	330	± 90	20	± 7	22	27	0.88	1.28

TABLE 2—Continued

No.	Name	z	FWHM		[OIII]		Equivalent width			[OIII]	FeII	
			H β				H β	[OIII]	FeII	H β	H β	
64	RX J1304.2+0502	0.229	1300	± 800	820	± 800	36	± 10	11	43	0.26	1.16
65	PG 1307+085	0.155	3860	± 220	360	± 65	70	± 2	30	19	0.38	0.28
66	RX J1314.3+3429	0.075	1240	± 140	260	± 120	56	± 1	13	39	0.21	0.78
67	RX J1319.9+5235	0.092	950	± 100	220	± 170	19	± 3	35	20	1.60	0.94
68	PG 1322+659	0.168	3100	± 370	130	± 130	63	± 4	6	25	0.10	0.43
69	IRAS 1334+2438	0.108	2800	± 180	900	± 100	47	± 3	7	55	0.14	1.25
70	Ton 730	0.087	3420	± 125	300	± 120	52	± 4	18	30	0.31	0.59
71	RX J1355.2+5612	0.122	1100	± 100	425	± 75	17	± 3	95	38	3.35	1.62
72	PG 1402+261	0.164	1623	± 145	710	± 100	75	± 5	2	72	0.02	1.10
73	RX J1413.6+7029	0.107	4400	± 1000	175	± 50	31	± 10	43	32	1.49	0.97
74	NGC 5548	0.017	6460	± 200	450	± 75	44	± 5	43	9	0.87	0.19
75	QSO 1421-0013	0.151	1500	± 150	630	± 350	69	± 3	12	44	0.14	0.70
76	Mkn 813	0.111	5940	± 1400	1100	± 470	38	± 5	14	10	0.31	0.26
77	Mkn 684	0.046	1260	± 130	170	± 140	40	± 1	5	52	0.12	1.50
78	Mkn 478	0.077	1630	± 150	575	± 70	52	± 1	9	46	0.17	0.97
79	PG 1448+273	0.065	1330	± 120	260	± 200	29	± 10	28	25	0.83	0.94
80	Mkn 841	0.036	6000	± 1500	150	± 130	64	± 20	53	13	0.77	0.21
81	SBS 1527+564	0.100	2760	± 420	200	± 150	70	± 5	213	55	3.31	0.70
82	Mkn 493	0.032	800	± 100	280	± 130	17	± 5	6	21	0.31	1.16
83	Mkn 876	0.129	7200	± 2000	540	± 60	67	± 8	17	19	0.25	0.31
84	RX J1618.1+3619	0.034	950	± 100	200	± 150	10	± 5	9	13	0.76	1.14
85	KUG 1618+40	0.038	1820	± 100	220	± 150	48	± 5	33	40	0.53	0.67
86	PG 1626+554	0.133	3460	± 1750	500	± 500	62	± 20	3	33	0.05	0.50
87	EXO 1627+4014	0.272	1450	± 200	200	± 140	63	± 10	23	31	0.35	0.49
88	RX J1702.5+3247	0.164	1680	± 140	1110	± 100	69	± 5	7	63	0.08	0.98
89	II Zw 136	0.065	2210	± 250	460	± 60	65	± 2	16	38	0.23	0.63
90	RX J2146.6-3051	0.075	3030	± 250	400	± 60	76	± 4	138	28	1.75	0.35
91	ESO 404-G029	0.063	6100	± 300	280	± 80	35	± 5	20	14	0.55	0.41
92	NGC 7214	0.023	4700	± 250	530	± 80	22	± 3	13	18	0.57	0.87
93	RX J2216.8-4451	0.136	1630	± 130	700	± 50	54	± 2	18	58	0.29	1.13
94	RX J2217.9-5941	0.160	1430	± 60	900	± 40	37	± 5	11	49	0.27	0.96
95	PKS 2227-399	0.318	3710	± 1500	380	± 50	58	± 15	207	23	3.60	0.39
96	RX J2242.6-3845	0.221	1900	± 200	380	± 90	69	± 2	24	63	0.31	1.01
97	RX J2245.2-4652	0.201	2250	± 300	740	± 60	55	± 6	28	31	0.44	0.59
98	RX J2248.6-5109	0.102	2350	± 330	260	± 30	53	± 5	61	18	1.07	0.34
99	MS 2254-36	0.039	1530	± 120	510	± 60	47	± 3	20	24	0.41	0.53
100	RX J2258.7-2609	0.076	2030	± 180	300	± 40	67	± 10	95	35	1.39	0.48
101	RX J2301.6-5913	0.149	7680	± 1500	630	± 40	60	± 10	20	7	0.35	0.12
102	RX J2301.8-5508	0.140	1750	± 200	280	± 70	39	± 5	5	54	0.12	1.55
103	RX J2304.6-3501	0.042	1450	± 100	250	± 40	31	± 5	81	31	2.39	0.91
104	RX J2312.5-3404	0.202	4200	± 950	390	± 50	33	± 7	29	7	0.75	0.22
105	RX J2317.8-4422	0.132	1010	± 150	330	± 60	45	± 2	14	50	0.28	1.09
106	RX J2325.2-3236	0.216	3010	± 300	120	± 120	86	± 15	60	23	0.50	0.23
107	IRAS 23226-3843	0.036	9500	± 4500	320	± 100	37	± 10	6	15	0.16	0.45
108	MS23409-1511	0.137	1030	± 100	690	± 50	32	± 6	7	35	0.18	1.18
109	RX J2349.4-3126	0.135	4200	± 2000	500	± 40	39	± 15	27	18	0.68	0.48
110	AM 2254-304	0.033	2400	± 200	250	± 100	32	± 7	3	24	0.09	0.81

FWHM are given in km s^{-1} and the equivalent widths are given in \AA .

TABLE 3

X-RAY SPECTRAL INDEX α_X , LUMINOSITIES, AND X-RAY VARIABILITY PARAMETER χ^2/ν OF THE SOFT X-RAY AGN SAMPLE

No.	Name	α_X	$\log L_X$	$\log \lambda L_{5100}$	$\log L_{bol}$	$\log L_{H\beta}$	χ^2/ν
1	Mkn 335	2.10	36.73	36.63	38.21	34.87	2.92
2	ESO 242-G008	1.56	36.54	36.56	37.45	34.69	2.31
3	Ton S 180	1.89	37.13	37.27	38.71	35.22	3.47
4	QSO 0056-36	1.72	37.50	37.93	39.30	35.95	1.48
5	RX J0100.4-5113	1.73	36.91	36.86	38.04	34.82	1.04
6	RX J0105.6-1416	1.29	37.11	36.86	38.48	35.02	1.24
7	RX J0117.5-3826	2.09	37.90	37.45	39.07	35.50	1.24
8	MS 0117-28	2.27	37.97	38.18	39.49	36.21	1.07
9	RX J0128.1-1848	1.55	36.37	36.20	37.09	34.14	1.04
10	IRAS F01267-217	1.43	36.97	37.22	38.31	35.41	1.17
11	RX J0148.3-2758	2.12	38.20	37.45	38.71	35.71	1.36
12	RX J0152.4-2319	1.67	37.18	37.38	38.47	35.51	1.64
13	Mkn 1044	1.74	36.23	36.16	37.20	34.24	2.48
14	Mkn 1048	1.53	36.71	36.80	38.25	35.04	1.92
15	RX J0311.3-2046	1.47	36.56	36.94	38.06	34.91	0.54
16	RX J0319.8-2627	1.79	36.91	36.92	37.86	34.95	1.86
17	RX J0323.2-4931	2.03	37.00	36.58	37.62	34.72	3.13
18	ESO 301-G013	2.01	36.76	36.75	37.75	34.97	1.24
19	VCV 0331-373	1.59	36.60	36.53	37.68	34.69	1.10
20	RX J0349.1-4711	2.45	37.61	37.68	39.25	35.89	2.14
21	Fairall 1116	2.48	37.29	36.94	38.00	35.12	1.63
22	ESO 359-G019	1.41	37.13	36.42	37.53	34.60	2.00
23	RX J0412.7-4712	1.66	37.24	37.46	38.23	35.45	2.24
24	1H 0419-577	2.20	37.83	37.87	39.38	36.00	1.33
25	Fairall 303	1.51	36.32	36.10	37.25	34.50	2.81
26	RX J0437.4-4711	2.09	36.60	36.84	38.01	34.83	1.19
27	RX J0439.6-5311	2.39	37.72	37.31	38.97	34.60	1.32
28	H 0439-272	1.51	36.91	37.12	37.92	35.13	1.48
29	1 ES 0614-584	2.46	36.92	36.26	37.45	34.04	3.24
30	RX J0859.0+4846	1.46	36.94	36.91	38.18	35.17	1.14
31	RX J0902.5-0700	2.17	37.14	36.34	37.86	34.59	1.15
32	Mkn 110	1.29	36.53	36.64	37.61	34.86	2.02
33	PG 0953+414	1.65	37.78	38.14	39.39	36.29	1.05
34	RXJ1005.7+4332	1.81	37.37	37.50	38.86	35.39	1.16
35	RX J1007.1+2203	1.68	36.97	36.49	38.11	34.30	2.55
36	CBS 126	1.65	37.08	37.32	38.57	35.45	1.88
37	HS 1019+37	0.98	37.37	36.95	37.73	34.76	1.48
38	Mkn 141	1.53	36.01	36.60	37.51	34.46	2.26
39	Mkn 142	1.88	36.57	36.51	37.56	34.53	3.18
40	RX J1034.6+3938	2.38	36.74	36.18	37.53	33.64	1.85
41	RX J1117.1+6522	1.89	37.06	37.29	38.59	35.38	2.97
42	PG 1115+407	2.05	37.29	37.51	38.83	35.60	0.97
43	Ton 1388	1.65	37.56	38.08	39.64	36.36	1.98
44	EXO 1128+69	1.60	36.64	36.54	37.55	34.32	2.03
45	B2 1128+31	1.43	37.94	37.72	38.80	35.65	1.18
46	SBS 1136+579	1.54	36.92	36.60	37.80	34.46	1.07
47	Z 1136+3412	1.81	36.20	35.96	37.12	34.00	3.52
48	Was 26	1.43	37.09	36.85	38.24	34.80	1.53
49	CASG 855	1.40	36.56	36.00	37.33	33.65	1.21
50	Mkn 1310	1.39	35.84	35.62	36.77	33.55	1.82
51	NGC 4051	1.62	34.29	34.57	35.55	32.40	18.5
52	GQ Com	1.18	37.42	37.40	38.26	35.44	1.54
53	RX J1209.8+3217	3.18	36.97	36.74	37.97	34.87	0.78
54	PG 1211+143	2.00	37.41	37.42	38.95	35.66	1.76
55	Mkn 766	1.77	36.21	36.31	37.23	33.79	8.86
56	3C 273	1.30	38.52	38.75	39.95	36.73	0.97
57	RX J1231.6+7044	1.38	37.89	37.10	38.53	35.10	1.22
58	Mkn 771	1.83	36.60	36.58	37.84	34.81	1.72
59	CBS 150	2.13	37.62	37.59	39.17	35.70	1.47
60	MCG+08-23-067	1.38	35.88	35.81	37.27	33.11	1.34
61	NGC 4593	1.47	35.74	35.45	36.53	33.73	0.20
62	IRAS F12397+3333	2.02	36.39	36.36	37.64	34.12	1.93
63	PG 1244+026	1.79	36.63	36.36	37.75	34.08	1.53
64	RX J1304.2+0502	2.38	37.66	37.40	39.02	35.31	5.08

TABLE 3—Continued

No.	Name	α_X	$\log L_X$	$\log \lambda L_{5100}$	$\log L_{bol}$	$\log L_{H\beta}$	χ^2/ν
65	PG 1307+085	1.58	37.41	37.52	39.08	35.78	0.87
66	RX J1314.3+3429	1.88	36.56	36.80	37.93	34.89	3.42
67	RX J1319.9+5235	1.60	36.84	36.45	37.51	34.09	3.37
68	PG 1322+659	2.07	37.51	37.71	38.81	35.87	1.52
69	IRAS 1334+2438	1.88	37.48	37.64	38.37	35.68	1.74
70	Ton 730	1.83	36.61	36.75	37.94	34.84	2.43
71	RX J1355.2+5612	1.93	37.04	36.98	37.60	33.83	2.27
72	PG 1402+261	1.83	37.36	37.72	39.17	35.99	0.71
73	RX J1413.6+7029	1.40	37.19	36.80	37.60	34.63	1.70
74	NGC 5548	1.33	36.40	36.56	37.53	34.61	1.27
75	QSO 1421-0013	1.72	37.48	37.34	38.76	35.56	2.34
76	Mkn 813	1.64	37.30	37.28	38.95	35.28	1.41
77	Mkn 684	1.36	36.23	36.87	38.35	34.81	1.75
78	Mkn 478	2.08	37.45	37.46	38.88	35.53	3.71
79	PG 1448+273	1.52	36.87	37.10	38.56	35.00	1.60
80	Mkn 841	1.50	36.28	36.64	37.79	34.85	1.00
81	SBS 1527+564	1.46	37.01	36.41	37.86	34.69	1.34
82	Mkn 493	1.57	36.03	36.74	37.63	34.33	2.03
83	Mkn 876	1.67	37.52	37.76	38.85	35.94	1.75
84	RX J1618.1+3619	1.54	36.12	35.71	36.79	33.09	2.49
85	KUG 1618+40	1.52	35.96	35.81	37.16	33.68	1.87
86	PG 1626+554	1.79	37.26	37.54	38.88	35.74	1.17
87	EXO 1627+4014	2.25	37.61	37.41	38.90	35.56	1.17
88	RX J1702.5+3247	2.13	37.47	37.29	39.22	35.51	1.29
89	II Zw 136	2.10	37.34	37.15	38.86	35.35	1.39
90	RX J2146.6-3051	1.59	36.92	36.72	37.61	35.00	1.62
91	ESO 404-G029	1.37	36.77	36.77	37.52	34.64	1.78
92	NGC 7214	1.34	35.81	36.30	37.22	33.96	1.84
93	RX J2216.8-4451	2.48	37.59	37.17	38.55	35.27	1.76
94	RX J2217.9-5941	2.69	37.58	37.14	38.60	35.06	4.20
95	PKS 2227-399	1.00	37.92	37.24	38.43	35.39	1.14
96	RX J2242.6-3845	2.19	37.42	37.03	38.50	35.23	0.89
97	RX J2245.2-4652	2.55	37.88	37.79	39.02	35.94	1.52
98	RX J2248.6-5109	1.95	37.47	37.35	38.33	35.46	1.23
99	MS 2254-36	1.78	36.51	36.34	37.27	34.33	2.34
100	RX J2258.7-2609	1.50	36.83	36.74	37.62	34.97	0.52
101	RX J2301.6-5913	1.65	37.69	37.35	38.30	35.49	1.03
102	RX J2301.8-5508	2.09	37.33	37.38	38.47	35.33	2.27
103	RX J2304.6-3501	1.65	36.16	36.08	37.08	33.98	1.94
104	RX J2312.5-3404	1.34	37.48	37.51	39.20	35.47	2.70
105	RX J2317.8-4422	2.87	37.17	36.77	38.89	34.83	0.79
106	RX J2325.2-3236	1.92	37.47	37.36	38.78	35.75	0.27
107	IRAS 23226-3843	1.20	36.43	36.43	36.88	34.27	0.93
108	MS23409-1511	2.03	37.39	37.42	38.52	35.28	1.66
109	RX J2349.4-3126	1.67	37.11	37.17	38.00	35.09	0.80
110	AM 2254-304	1.30	35.95	36.18	36.87	34.00	1.62

All luminosities are given in units of Watts.

Fig. 11.— Optical spectra of the soft X-ray selected sample which have not been published yet (see Table 1). The wavelength is given in units of \AA and the flux density is given in units of $10^{-19} \text{ W m}^{-2} \text{\AA}^{-1}$. All spectra are shown in the observed frame. **Please note:** this is a special version for astro-ph that does not contain the optical and FeII subtracted spectra. The complete paper including the spectra can be retrieved from http://www.astronomy.ohio-state.edu/~dgrupe/research/sample_paper1.html

Fig. 12.— FeII-subtracted spectra, the wavelength is given in units of \AA and the flux density is given in units of $10^{-19} \text{ W m}^{-2} \text{\AA}^{-1}$. The dotted line marks the zero line of the FeII template. **Please note:** this is a special version for astro-ph that does not contain the optical and FeII subtracted spectra. The complete paper including the spectra can be retrieved from http://www.astronomy.ohio-state.edu/~dgrupe/research/sample_paper1.html

TABLE 4
MEAN, STANDARD DEVIATION, AND MEDIAN OF THE WHOLE SAMPLE (110 SOURCES), NLS1s (51), AND
BLS1s (59).

Property	all sources (110)			NLS1s (51)			BLS1s1 (59)		
	Mean	σ	Median	Mean	σ	Median	Mean	σ	Median
FWHM($H\beta$)	2695	1760	2210	1380	350	1450	3830	1700	3100
FWHM([OIII])	431	255	370	445	280	345	420	240	390
EW($H\beta$)	48	19	47	45	21	47	50	17	47
EW([OIII])	32	37	20	24	32	16	38	40	23
EW(FeII)	30	15	28	38	15	38	23	12	22
[OIII]/ $H\beta$	0.71	0.82	0.36	0.66	0.91	0.29	0.75	0.74	0.50
FeII/ $H\beta$	0.73	0.42	0.65	0.99	0.40	0.96	0.50	0.28	0.48
α_X	1.77	0.39	1.67	1.96	0.41	1.93	1.62	0.30	1.56
$\log L_X$	36.99	0.64	37.04	36.94	0.71	37.00	37.03	0.57	37.09
$\log \lambda L_{5100}$	36.93	0.64	36.91	36.81	0.66	36.80	37.03	0.61	36.94
$\log L_{bol}$	38.13	0.78	38.06	38.10	0.82	38.11	38.15	0.74	38.06
$\log L_{H\beta}$	34.92	0.81	34.97	34.76	0.81	34.86	35.05	0.79	35.04
$\log L_{[OIII]}$	34.53	0.73	34.54	34.29	0.63	34.36	34.74	0.75	34.84
$\log L_{FeII}$	34.70	0.79	34.66	34.72	0.79	34.87	34.68	0.79	34.65
z	0.107	0.075	0.083	0.113	0.088	0.082	0.101	0.061	0.084
χ^2/ν	1.95	1.92	1.60	2.57	2.65	1.94	1.43	0.50	1.41

The FWHM are given in units of km s^{-1} , the rest frame equivalent widths in \AA , and the luminosities are given in units of Watts.